Photochemistry Studied with *Ab Initio* Orbital-Correlation and State-Correlation Plots: Classic Cyclobutene Ring Opening, and the Reaction of N_2 with Photoexcited O_2

HUANCONG SHI, DAVID C. ROETTGER, ALLAN L. L. EAST
Department of Chemistry and Biochemistry, University of Regina, Regina, Saskatchewan S4S 0A2, Canada

Received 26 July 2007; Revised 27 August 2007; Accepted 28 August 2007
DOI 10.1002/jcc.20843
Published online 26 October 2007 in Wiley InterScience (www.interscience.wiley.com).

Abstract: Pericyclic reaction theory arose from ideas presented in 1965, based on orbital-energy correlation diagrams (Woodward and Hoffmann) and state-energy correlation diagrams (Longuet-Higgins and Abrahamson). Here we have used *ab initio* complete-active-space self-consistent field (CASSCF) calculations to generate such diagrams. First we present diagrams for the classic case of cyclobutene ring opening, to demonstrate agreement between the CASSCF results and the classic diagrams of both Woodward/Hoffmann and Longuet-Higgins/Abrahamson. Then we present diagrams for the more difficult cases of N_2 + photoexcited O_2, to produce either 2 NO or NNO + O. These N_2 + O_2 cases feature significant electron reorganization, for which elementary pencil-and-paper diagrams are less accurate. Finally, the benefits and limitations of such diagrams for predicting photochemistry are briefly discussed.

 J Comput Chem 29: 883–891, 2008

Key words: photochemistry; state correlations; orbital correlations; cyclobutene; N_2O_2

Introduction

Pericyclic reaction theory advanced in great strides during the mid 1960s and 70s, spurred on by Woodward and Hoffmann's symmetry-minded approach. Their orbital correlation diagrams and subsequent selection rules led the way for themselves and others to examine the unusually high level of stereospecificity of these reactions. Initially in 1965, after a preliminary communication regarding the symmetry of the highest-occupied molecular orbital,[1] the *orbital correlation diagram* idea of Woodward and Hoffmann (WH)[2] appeared, immediately preceded by an alternative *state correlation diagram* idea of Longuet-Higgins and Abrahamson (LA),[3] in consecutive articles. These early works mainly focused on using these qualitative correlation plots to draw conclusions without engaging in extensive computations.[4]

There are, however, many "nonstandard" reactions that are not easily handled by the summary results of pericyclic reaction theory, and quantum chemistry computations may shed light on such cases. For thermally induced reactions, where a molecular system adiabatically follows a ground-state pathway, quantum chemistry tools such as transition-state optimization and steepest-descent path-following are well-honed. For photochemical reactions, however, the situation is not so simple, due to excited-state crossings. The first difficulty is that most quantum chemistry techniques have problems following an adiabatic excited-state pathway, i.e., maintaining convergence on one excited-state potential-energy-surface path, when other states are nearby in energy. The second difficulty is that many photochemical reactions, as they proceed from a photoexcited initial state to a ground-state product, invoke nonadiabatic steps.

To make progress in examining photochemical reactions, we sought to tackle the first of these two difficulties. We have used quantum chemistry calculations to generate both orbital-correlation and state-correlation diagrams, for a classic case and two complex ones, to see if such diagrams could be useful for studying the more complex cases. Such calculations for excited states are quite rare, because orbital-energy calculations tend to be state-dependent, and state-energy calculations have convergence difficulties; we present ways to compute a more general orbital-correlation plot and a more continuous state-correlation plot. The best previous attempt to generate similar plots might be by Buenker et al. in 1971,[5] whose article presents computed *state-specific* orbital-correlation plots for allowed transitions only.

The classic example we chose for testing purposes was the ring-opening conversion of cyclobutene to *cis*-1,3-butadiene, the

This article contains supplementary material available via the Internet at http://www.interscience.wiley.com/jpages/0192-8651/suppmat

Correspondence to: A. L. L. East; e-mail: allan.east@uregina.ca

Contract/grant sponsor: NSERC (Canada)

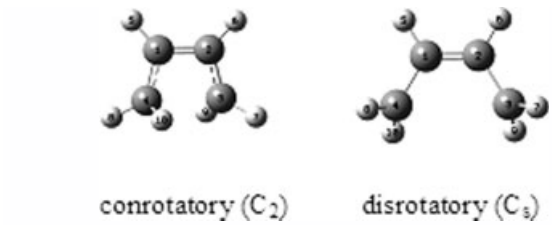

Figure 1. Transition states for the two ring-opening paths of cyclobutene → butadiene.

first reaction discussed by both WH[1] and LA.[3] In this reaction, the conrotatory (C_2-symmetry) pathway is thermally allowed, while the disrotatory (C_s-symmetry) pathway is thermally forbidden but photochemically allowed (Fig. 1). The WH explanation for the two different pathways is that the molecular *orbitals* of reactants and products correlate differently in the two cases: in the conrotatory orbital-correlation diagram, the occupied-orbital energies do not cross any unoccupied-orbital energies, but in the disrotatory diagram, the HOMO and LUMO orbital energies cross (and do not mix). Alternatively, the original LA explanation is that the electronic *states* of reactants and products correlate differently in the two path cases (Fig. 2); in their conrotatory state-correlation diagram, the ground states correlate with each other, but in the disrotatory diagram, the ground-state energy rises toward an avoided crossing (creating a barrier for the thermal reaction), while the first excited states of reactant and product correlate with each other (hence photochemically allowed).

The other two reactions of interest are hypothetical photochemical reactions of UV-excited $B^3\sum_u^-$ state O_2 with ground-state N_2 to produce either 2 NO or NNO + O. These are theoretically complex because they involve great number of orbitals and states changing in small ranges. Excluding atomic 2s and Rydberg orbitals, the orbital correlation diagrams might include as many as 14 electrons in 12 orbitals, making it significantly more complex than the C_4H_6 system. These high densities of orbitals and states would likely lead to a great deal of repulsion due to avoided crossings, making elementary "pencil-and-paper" correlation diagrams more inaccurate.

Our interest in these hypothetical N_2 + O_2 photoreactions was motivated by the experiments of Zipf and Prasad,[6,7] that have produced N_xO_y from UV irradiation of mixtures of N_2 and O_2. In 1998 they reported production of odd-nitrogen oxides (either NO or NO_2) from 185 nm (647 kJ mol^{-1}) irradiation,[6] and in 2000 they reported NNO production from 170 to 200 nm (600–700 kJ mol^{-1}) irradiation.[7] These authors speculated that their observed products result from direct reactions with the $B^3\sum_u^-$ state of O_2, the state responsible for the Schumann-Runge absorption band (T_e = 591 kJ mol^{-1}), either in free collision or starting from an $N_2 \cdot O_2$ complex. Donaldson[8] has already presented an orbital correlation plot and used it to suggest that N_2 + $B^3\sum_u^-$ O_2 cannot form two ground-state NO molecules; we can evaluate his orbital predictions. We will also check to see if our diagrams can provide agreement with the observation of very small amounts of NNO produced by the lower-energy photoreaction N_2 + $A^3\sum_u^+$ O_2 (T_e = 427 kJ mol^{-1}), as demonstrated by Slanger and coworkers[9] (243–250 nm, 478–492 kJ mol^{-1}) and by Wine and coworkers[10] (266 nm, 450 kJ mol^{-1}). The applicability of correlation diagrams to polyatomic photochemical problems is, however, somewhat limited, as will be discussed.

Theoretical Methods

Cyclobutene Ring Opening

First, reaction paths were needed. We generated quadratic synchronous transit (QST) internal-coordinate paths for both conrotatory (C_2 symmetry) and disrotatory (C_s symmetry) pathways, by using Lagrange interpolating polynomials to fit through three optimized points for each path: the C_{2v}-symmetry reactant (point 1) and product (point 9), and the thermal (ground-state) transition state (point 5). Note that the butadiene product was restricted to C_{2v} symmetry (the actual minimum structure is slightly conrotated at this level of theory), and the disrotatory (C_s) transition state was restricted to C_s symmetry (the actual transition state appears to be distorted into C_1 symmetry). The transition state geometry optimizations were performed with the OPT=(TS,EF) algorithm[11] of the GAUSSIAN03 software package,[12] at the CASSCF[13](4,4)/cc-pVDZ[14] level of theory, using direct analytic MCSCF gradients.[15,16] The CASSCF active space was selected to include the four molecular orbitals involved in the reaction according to both WH and LA, namely the π and π^* of cyclobutene and the σ and σ^* of the bond to be broken.[3] The default orbital guess worked well, except for cyclobutene, where single point runs and orbital swapping was required to correct the active spaces. The paths, presented as sets of internal coordinate values, appear in supplementary material (available via the journal: four tables depicting the reaction paths chosen in this study).

For orbital energy plots, a strategy was needed to compute an orbital energy consistenly, regardless of occupation. A high-spin model was selected in which only the core orbitals are doubly occupied and all the valence orbitals are singly occupied; for hydrocarbons this leaves the molecule neutrally charged. The orbital energies were computed with GAUSSIAN03 at both ROHF/STO-3G and ROHF/cc-pVDZ levels of theory.[12] The resulting plots were quite similar, so only the ROHF/cc-pVDZ results are presented here. The default orbital guess worked well, except for the butadiene end point (a different high-spin state was obtained); this problem was cured by starting each

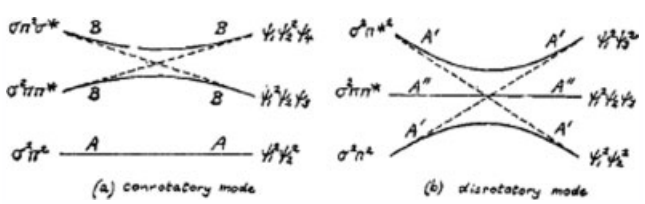

Figure 2. The original state correlation plots of Longuet-Higgins and Abrahamson[3] for cyclobutene → butadiene (Reproduced with permission, Copyright 1965 American Chemical Society).

self-consistent field calculation with the converged orbitals from the previous path point.

The state energies were calculated with the MOLPRO 2002.6[17] implementation of CASSCF[18,19](4,4)/cc-pVDZ, using the state-averaging algorithm (all 20 singlet states that can arise from the active space). Initial guesses for orbitals were taken from a converged set from a neighboring path point (primarily to ensure the correct active space), before starting each 20-state-average CASSCF run. Despite this precaution, the desired active space could not be achieved for the butadiene structure, points eight and nine, of the conrotatory pathway, because an orbital rotation of the active 9 A orbital with the 11 A orbital occurred (partial mixing at point 8, complete replacement at point 9). We believe this is due to state-averaging: some of the states that initially arose by filling the 9th A orbital were probably of higher energy than others which would occupy 11th A instead, and despite the two orbitals being orthogonal at point 9 (they have different symmetries in C_{2v}), the algorithm somehow managed to pull 11th A into the active space. This problem did not occur on the disrotatory pathway because the two orbitals are of differing symmetry; the active space with MOLPRO was defined to have exactly two orbitals of each symmetry.

$N_2 + O_2$

Four reaction paths were considered, as depicted in Figure 3: (i) side-on (C_{2v}) attack to form 2 NO, (ii) crosswise (C_2) attack to form 2 NO, (iii) end-on ($C_{\infty v}$) attack to form NNO + O, and (iv) angled (C_s) attack to form NNO + O.

QST paths are less appropriate for bimolecular reactions, in which changes in internal coordinate values are slow during approach and more sudden during collision. Furthermore, there was also no obvious way to optimize a midpoint for each of these four pathways. Hence, the pathways were arbitrarily constructed, using mathematical functional forms for time-dependent Cartesian coordinates of each atom, in a way that appeared likely to approximate realistic synchronized movement of the atoms. The dimensionless time parameter t was chosen so that

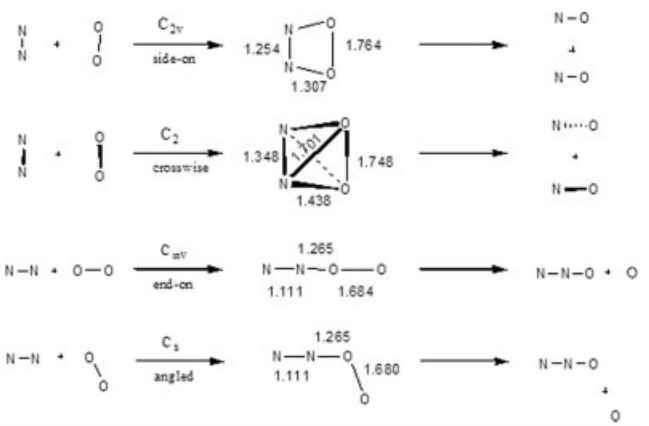

Figure 3. The pathways chosen for investigation of $N_2 + O_2$, including the bond lengths (in Å) used for the middle structures in each case. The complete paths are provided in supplementary material.

$t = -\infty$ represented infinitely separated reactants, $t = +\infty$ represented infinitely separated products, and $t = 0$ represented the structure of closest approach. Ground-state experimental bond lengths were chosen for asymptotic structures, except for the O_2 reactant which was chosen to begin from its experimental B-state bond length.[29,30] The functions for each Cartesian coordinate for each pathway appear in supplementary material.

For orbital energy plots, the high-spin model requires single-electron occupation of all 16 valence orbitals. This could be done in two ways: by removing six electrons ($N_2O_2^{6+}$), or by substituting carbon atoms for N and O. The former resulted in large dips in orbital energies for the $t = 0$ region; thus, carbon atoms were used in the computations. The drawback in using carbon atoms is that orbital ordering might be compromised, particularly the σ_{2p} and π_{2p} orbitals of NO which became reversed, but this was deemed a small qualitative defect that has no bearing on diabatic orbital correlations. The orbital energies were computed with GAUSSIAN03 at the ROHF/STO-3G levels of theory, but default initial guesses were only used at $t = 0$ geometries; from here, we employed a "push method" outward, where orbital guesses for a particular path point were the converged orbitals from the previous path point. A minimal basis set was used because ROHF/cc-pVDZ calculations did not appear to maintain the desired high-spin occupancies throughout.

The state energies were calculated at the CASSCF(14,12)/cc-pVDZ level of theory, using the MOLPRO 2002.6 state-averaging algorithm as we did for cyclobutene ring opening. For N_2 + O_2 reactions, we requested 12 triplet states, since both the ground and B states of O_2 are triplet states, and because 12 is an appropriate number for the 2 NO dissociation asymptote, which leads to four degenerate triplet states from X NO + X NO,[20] and eight degenerate triplet states from X NO + B NO.[21] The state correlation calculations were challenging, not only to achieve convergence at all geometries, but to obtain consistent sets of adiabatic triplet states in the state-averaging. A "push method" of orbital and state guesses in the forward direction (t from $-\infty$ to $+\infty$) often led to different states than a "push method" run in the reverse direction. This turned out to be a useful check, to reveal cases where we were unsuccessful in obtaining the lowest adiabatic states in each symmetry block. Reverse pushes from products to reactants generally worked the best, but for path (i) we had to splice results from both runs ("left-to-centre" and "right-to-centre").

Results and Discussion

Cyclobutene Ring Opening

Figure 4 presents the computed orbital correlation diagrams for both the C_2 and C_s symmetry paths. The ground states of both cyclobutene and butadiene would have the lower 11 orbitals (below $\varepsilon = -0.2$) doubly occupied and the upper 11 orbitals unoccupied. The four orbitals of the classic WH diagrams are highlighted in both plots, and the crucial features are indeed reproduced: the conrotatory path plot shows the crossings of HOMO with HOMO−1 and LUMO with LUMO+1, and the disrotatory plot shows the crossing of the HOMO with the

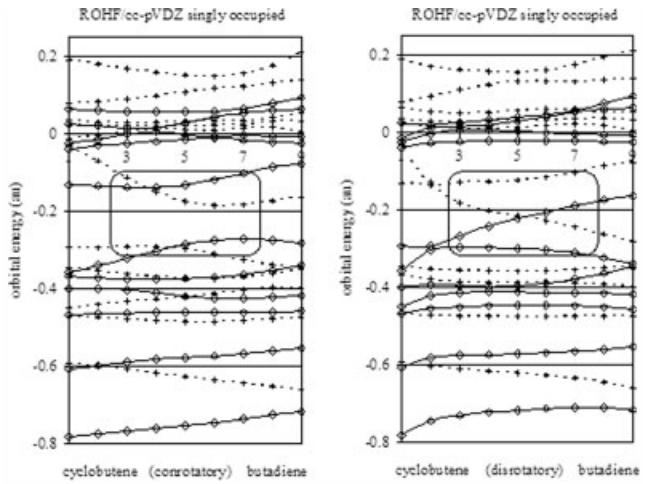

Figure 4. Orbital energy plots for cyclobutene → butadiene: valence orbital energies versus course of reaction, with the important regions highlighted. Left plot: conrotatory (C_2) path, solid/dashed lines for orbitals of a/b symmetry, respectively. Right plot: disrotatory (C_s) path, solid/dashed lines for orbitals of a′/a″ symmetry, respectively.

LUMO. The disrotatory plot also shows avoided crossings between orbitals of same symmetry near the cyclobutene initial geometry, which are ignored in textbook plots.

Figure 5 presents the state correlation plots, for all 20 states that arise from the CASSCF(4,4) active space. For the conrotatory plot, the active-space problems for points 8 and 9 (see Theoretical Methods) was solved by omitting data for point 8 and replacing the data for point 9 with that from the C_s-symmetry (disrotatory path) calculation. The comparison to the LA plots requires more careful inspection.

For the conrotatory path (left plot of Fig. 5), the LA plot (left plot of Fig. 2) featured a level A-symmetry ground state and an avoided crossing of two higher B states. In the computed results, the ground state is not perfectly level, with an activation energy of 0.036 au for the thermal reaction. The avoided crossing of the B states (dashed lines) can be seen in the highlighted region above $E = -154.6$ au, above two other A states that are absent from the LA plot. Pericyclic reaction theory predicts that photochemical conrotatory ring opening/closing is forbidden, but note that the computed results suggest that the opening is allowed (i.e. barrierless). This disagreement is actually correct, as the photochemical ring-opening of cyclobutenes is experimentally known to be somewhat nonstereospecific.[22,23]

For the disrotatory path (right plot of Fig. 5), the LA plot (right plot of Fig. 2) featured a level excited A″ state sandwiched by an avoided crossing of the ground A′ state with a higher A′ state. In the computed results, the avoided crossing of the A′ states is evident, but the energy gap is rather large, resulting in a ground-state activation energy of 0.065 au for the thermal reaction. The A″ state energy of cyclobutene (dashed line) is not perfectly level, and it does not remain sandwiched between the energies of the two A′ states throughout the reaction path. This early crossing of the A″ state with the 2nd A′ state was seen in primitive computational studies as far back as 1969 and 1975.[24,25]

The desired goal was successful; orbital-correlation and state-correlation plots could be generated. We should, however, address the issue of their usefulness in understanding photochemical reaction mechanisms. For the reverse reaction (disrotatory ring closure), the most popular modern-day description of the mechanism invokes two nonadiabatic internal conversion steps: the first from A″ down to spectroscopically dark 2A′, and the second from 2A′ to ground 1A′.[22–27] This mechanism arose from the discovery of conical intersections connecting each pair of states, either on or alongside the C_s-symmetry disrotatory pathway. This mechanism is impossible to predict, or even understand, using the orbital-correlation plots. The state-correlation plots have some limited usefulness, which we now describe. The disrotatory plot (right-hand plot of Fig. 5) does suggest an initial driving force for the disrotatory ring-closure direction. It also shows regions of "close contact" between pairs of states (point 8 for A″/2A′ and point 6 for 2A′/1A′) that are commensurate with the reaction-extent of the conical intersections. However, it appears very difficult to predict when a conical intersection or internal conversion will happen, given such plots.

Incidentally, an additional way to identify if a path might be thermally forbidden is to tally the orbital occupations of reactants and products by symmetry block. Table 1 does this for the six reactions studied here, including the two C_4H_6 ring-opening reactions. The disrotatory reaction is predicted to be theoretically forbidden, simply because it would require at least two electrons to change orbitals, namely an a′-symmetry pair to become an a″ symmetry pair. However, this test cannot identify thermally allowed paths; this is because it cannot predict whether a pair of electrons would need to

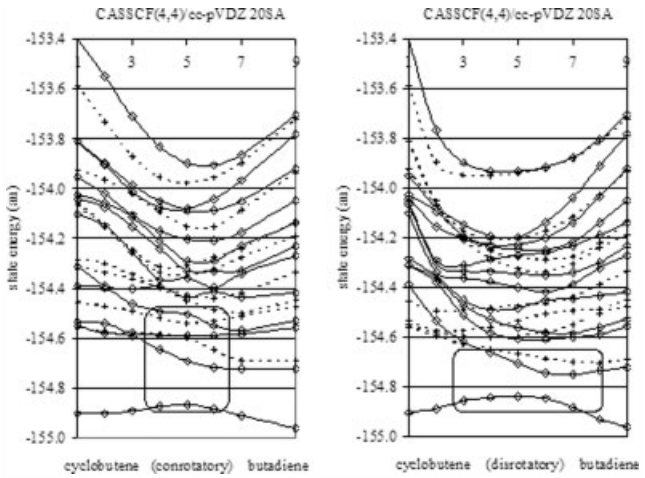

Figure 5. State energy plots for cyclobutene → butadiene: Twenty electronic state energies versus course of reaction, with the important regions highlighted. Left plot: conrotatory (C_2) path, solid/dashed lines for states of A/B symmetry, respectively. Right plot: disrotatory (C_s) path, solid/dashed lines for states of A′/A″ symmetry, respectively.

Table 1. Ground-State Valence Orbital Correlations by Symmetry Block.

Reaction	Orbital occupations, reactants	Orbital occupations, products	Thermally forbidden?
Cyclobutene→butadiene, C_s path	a'^{18}, a''^{12}	a'^{16}, a''^{14}	Yes
Cyclobutene→butadiene, C_2 path	a^{16}, b^{14}	a^{16}, b^{14}	Unclear
$N_2 + O_2 \rightarrow 2$ NO, C_{2v} path	a_1^{12}, b_1^4, b_2^5, a_2^1	a_1^8, b_1^2, b_2^8, $a_2^2 + 2$	Yes
$N_2 + O_2 \rightarrow 2$ NO, C_2 path	a^{13}, b^9	a^{10}, $b^{10} + 2$	Yes
$N_2 + O_2 \rightarrow$ NNO + O, $C_{\infty v}$ path	a^{12}, e^{10}	a^{11}, $e^{10} + 1$	Unclear
$N_2 + O_2 \rightarrow$ NNO + O, C_s path	a'^{17}, a''^5	a'^{16}, $a''^5 + 1$	Unclear

change orbitals within a symmetry block. An orbital correlation plot would be needed to judge this.

$N_2 + O_2 \rightarrow 2$ NO

The rudimentary analysis of orbital occupations in Table 1 proves what is well known, that the uncatalyzed reaction of nitrogen with oxygen to form 2 NO is thermally forbidden. The remaining question is, with O_2 excited to the B state, can it become photochemically allowed?

Figure 6 presents our theoretical pencil-and-paper orbital correlation plots for all 16 valence orbitals, for the two paths considered. For the lower-symmetry crosswise plot, many avoided crossings are predicted. Note that the asymptotic orbital energies for N_2, NO, and O_2 are taken to be the same, for simplicity. Donaldson, who attempted the C_{2v}-symmetry plot,[8] did not make such a simplification, instead making an undeclared choice for the orbital ordering. Further comparison of Donaldson's plot to ours reveal some puzzling aspects in the former, such as the differing number of orbitals on the left and right, and the consideration of only one of the four possible (degenerate) electronic states that can represent ground-state products. In any case, the more important observation is that neither predicted figure looks very similar to the computed plots, which appear in Figure 7. With careful comparison, one can see that many of our predicted avoided crossings are quite visible, but that orbital orderings on the left ($N_2 + O_2$) side of each plot are more complex than the simplified ordering presented in Figure 6. Hence, "pencil-and-paper" plots like Figure 6 are not as useful as one might hope.

Let us consider Figure 7 in some detail. The left-hand plot demonstrates that the side-on reaction is thermally forbidden, because of the rise in energy of three of the occupied σ_{2p} and π_{2p} orbitals (to become one σ^*_{2p} and two π^*_{2p} orbitals). The right-hand plot demonstrates that the crosswise reaction is also thermally forbidden, because one of these three orbitals must still rise in energy to become an antibonding orbital (after a large oscillation due to two avoided crossings). Now, the hypothesized photochemical reaction involves a $\pi_{2p} \rightarrow \pi^*_{2p}$ excitation on O_2, so that we would imagine three π^*_{2p} electrons and an electron hole in the π_{2p} orbitals. The side-on photochemical reaction is still clearly forbidden according to the left-hand plot, because five electrons would still have to rise in energy while the three π^*_{2p} electrons could fall. The crosswise reaction (right plot) may not be as clearly conclusive, but it shows that the three π^*_{2p} electrons here face energy barriers along this path, strongly suggesting that this route is also photochemically forbidden.

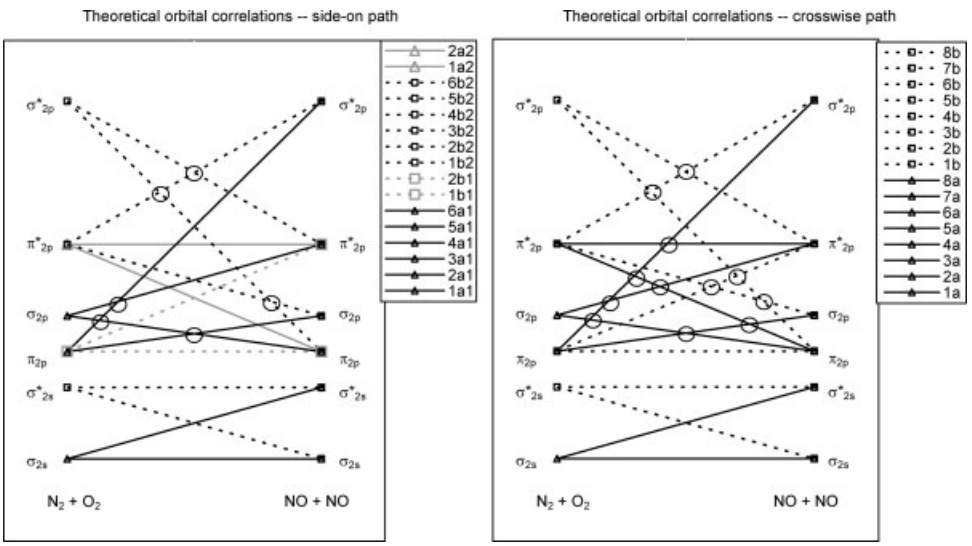

Figure 6. Theoretical orbital correlations for two different $N_2 + O_2 \rightarrow 2$ NO pathways. Circles denote predicted avoided crossings.

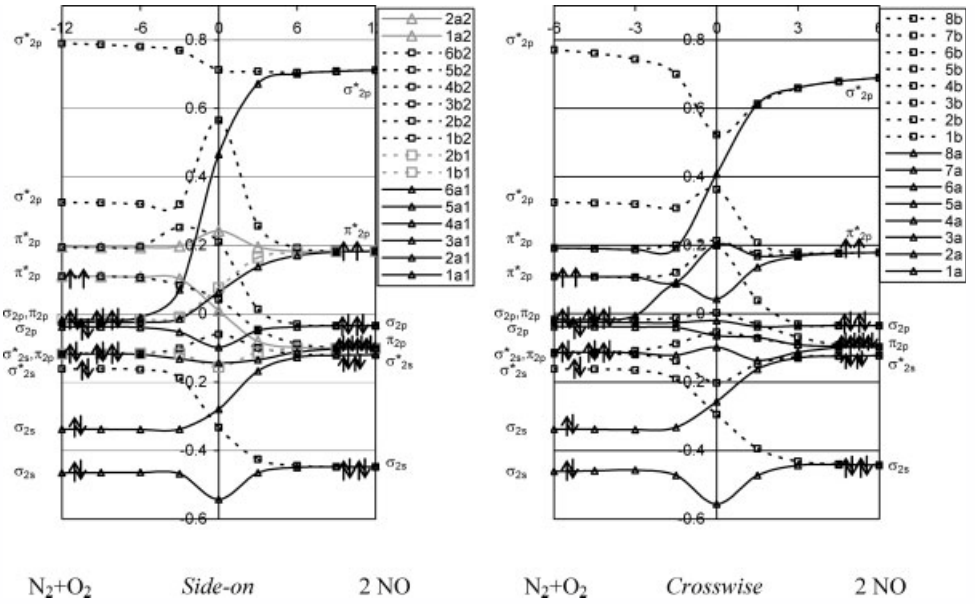

Figure 7. Computed orbital energies for two different $N_2 + O_2 \rightarrow 2$ NO pathways. The ground-state electron occupations are also pictured.

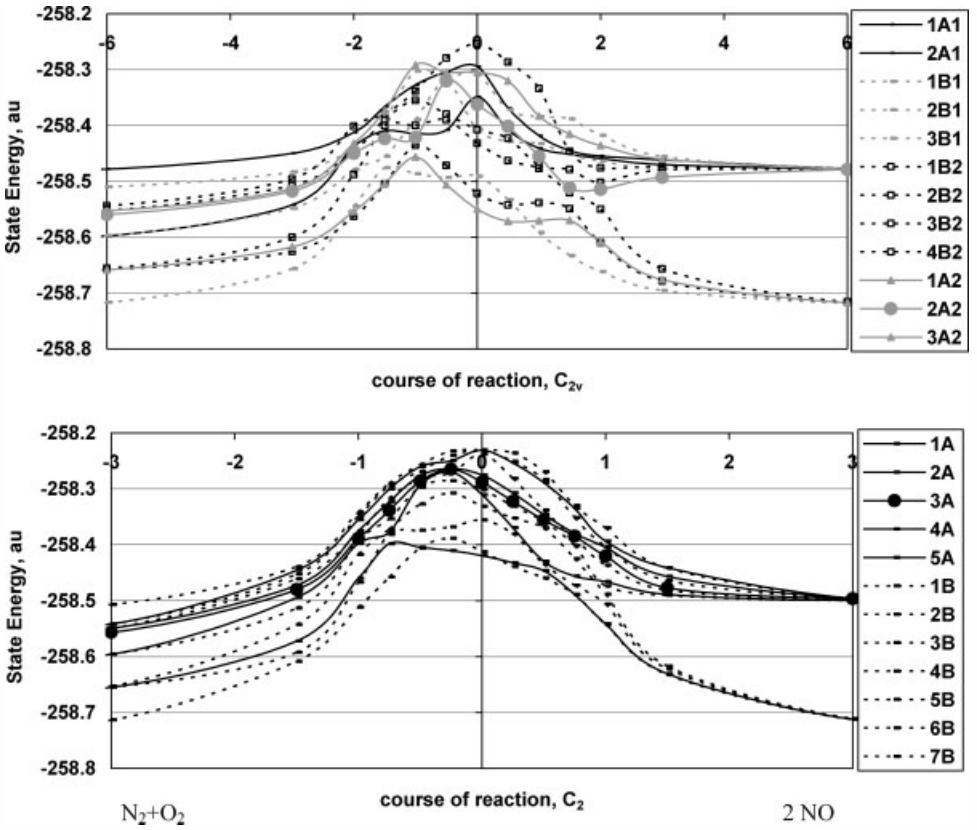

Figure 8. Computed state energies for two different $N_2 + O_2 \rightarrow 2$ NO pathways. In both plots, the photoexcited (adiabatic) state of interest is labeled with filled circles (B O_2).

The state correlation plots are presented in Figure 8. All 12 triplet states on the left-hand side are combinations of an O_2 triplet state with the ground singlet state of N_2; this is due to the stretched O—O bond, which reduces O_2 excitation energies, as well as the high photoexcitation energy of N_2. On the right side we have four degenerate states from X NO + X NO, and a higher set of eight from X NO + B NO, as mentioned in the Theoretical Methods section. The ground states of reactants and products are seen to be connected, but only due to avoided crossings which are difficult to see in the plot, and the thermal barriers are seen to be over 0.24 au (630 kJ mol^{-1}) along both paths, dramatically suggesting that the thermal reactions are indeed forbidden. For the photochemical reaction involving the B state of O_2 (filled circles in Fig. 8), the adiabatic pathway, whether side-on or crosswise approach, is clearly seen to feature a significant barrier en route to products. A diabatic course of the A_2 state in the upper plot, with a barrier of only 0.10 au (260 kJ mol^{-1}), can be imagined if the system can hop to the lower A_2-symmetry state at the avoided crossing at $x = -1$ ($E = -258.45$ au). This is still a large barrier.

The barriers in these plots are sensitive to the path trajectory, which we admit is somewhat difficult to choose. We did explore three different choices for the "$t = 0$" structure and found large barriers in all cases, but this is only suggestive at present.

The orbital-correlation and state-correlation plots appear to be useful. They suggest that the photochemical reaction, in the absence of nonadiabatic or Rydberg-state evolution during the reaction, is unlikely.

$$N_2 + O_2 \rightarrow NNO + O$$

For production of NNO + O, the rudimentary analysis of Table 1 cannot rule out even the thermal (ground state) reaction, and hence the correlation plots may prove even more useful.

The orbital correlation plots for both end-on and angled attack appear in Figure 9. For the end-on attack ($C_{\infty v}$, left-hand plot), the thermal reaction appears thwarted by a large energy barrier for one of the σ_{2p} orbitals. This barrier arises from an avoided crossing, which can be understood in an sp-hybridization framework: lone-pair sp hybrid orbitals on the second N and first O will run into each other, creating the σ and σ^* orbitals between these two atoms in NNO, and explaining the rise of one of these orbitals to a σ^* orbital on the right. The rise is not completed, due to the avoided crossing with an orbital that is originally the σ^* of O_2, but which correlates to a nonbonding orbital on one of the two O atoms. The barrier in this plot is 0.23 au (600 kJ mol^{-1}), offset only slightly by the lowering of energy of other electrons.

For the angled attack (right-hand plot of Fig. 9), an additional avoided crossing occurs that improves the plight of these σ_{2p}-orbital electrons, reducing their barrier substantially (to 0.08 au). Unfortunately, it also causes one of the two π^*_{2p} electrons of O_2 (the one in the a′ orbital) to face a new barrier (0.09 au) during the reaction, somewhat offsetting the benefits. The cumulative effects to evaluate the feasibility of thermal reaction are not as easy to discern in this plot.

For the π to π^* O_2 photoexcitation of interest, the left-hand plot suggests that this will improve the likelihood of the end-on reaction, because it removes an electron from a rising-energy π to a falling-energy π^* orbital. This does not appear to be enough to offset the larger barrier for the σ_{2p} electrons, although the net result becomes closer to the limit of accuracy of the approximations made in making this plot (namely, the use of carbon atoms, and the orbital approximation itself). In the right-hand plot, the same level of improvement is seen; please note that one component of the B state of O_2 allows the photoexcited electron to reside in the falling-energy a″ orbital of the originally π^*_{2p} degenerate pair.

Next we turn to the state correlation plots, in Figure 10. On the right-hand side of these plots, the ground state is triply degenerate because of the ^3P ground state of O atom; all product excited states appear at energies higher than the original photoexcitation energy (X N_2 + B O_2, the reactant state labeled with filled circles). The sizeable energy barriers for ground-state evolution lead us to conclude that the thermal reaction is forbidden, just as we concluded based on the orbital correlation diagrams. The power of the state plots becomes more impressive when considering the photochemical reaction, because they demonstrate, with greater clarity than the orbital plots, that the photochemical reaction from the B state of O_2 will not occur, if it proceeds adiabatically among these valence states: this state adiabatically correlates to higher-energy states of the products. However, nonadiabatic evolutions might be possible for either of these NNO-producing trajectories, because in both plots in Figure 10, a lower adiabatic state of the same symmetry evolves at energies lower than, or commensurate with, the original photoexcitation energy. This is unlike the situation in Figure 8, where the nonadiabatic-hop reaction requires a rise in energy.

Hence, photochemical production of NNO + O directly from X N_2 + B O_2 is plausible only if it occurs nonadiabatically.

We can also use Figure 10 to consider the lower-energy photoreaction X N_2 + A O_2 → NNO + O, shown by the groups of Slanger and coworkers[9] and Wine and coworkers,[10] to produce very little product. This initial state appears in Figure 10 labeled with open circles, initially at −258.66 au. Despite the favorable energy match of this initial state with the ground state products, our diagram for the most favorable approach (angled approach, the lower of the two plots) indicates a substantial energy barrier for this photochemical reaction, in accordance with the very low experimental yields.

Conclusions

Orbital-energy correlation diagrams and state-energy correlation diagrams can be computed *ab initio*, using artificially high-spin ROHF and state-averaged CASSCF calculations, respectively. Path selection was easier for the unimolecular case, but rather arbitrary for the bimolecular cases. The methods succeeded in reproducing the classic diagrams of both Woodward/Hoffmann and Longuet-Higgins/Abrahamson for the classic example of cyclobutene ring-opening. The state-correlation plots were the most useful for the examination of hypothetical N_2 + O_2 reactions, although there are difficulties in being able to predict nonadiabatic or asymmetric pathways.

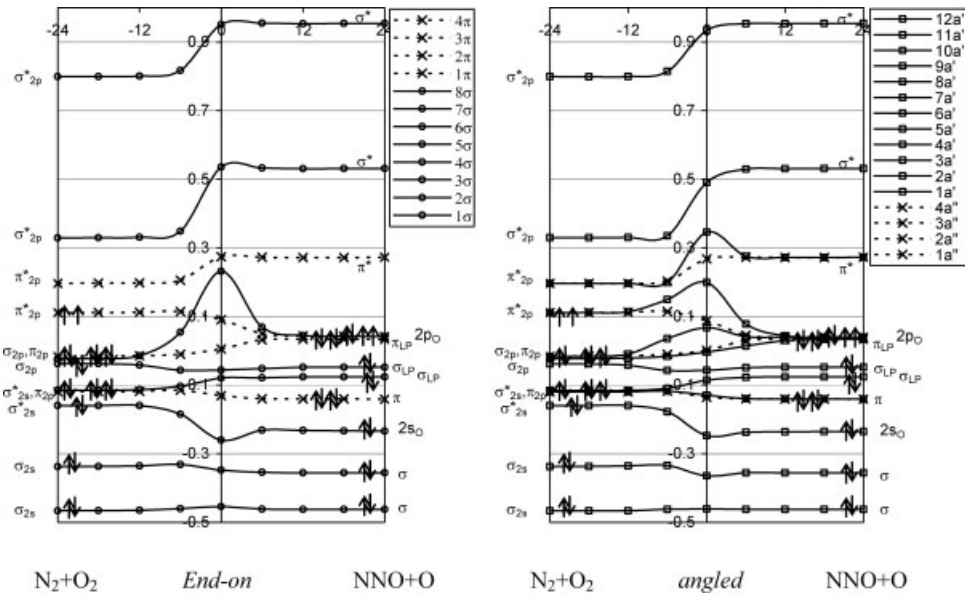

Figure 9. Computed orbital energies for two different $N_2 + O_2 \rightarrow NNO + O$ pathways. Left: end-on ($C_{\infty v}$) approach, with solid and dashed curves for σ and π symmetry, respectively. Right: angled (C_s) approach, with solid and dashed curves for a′ and a″ symmetry, respectively.

One can conclude, based on these diagrams, what is innately known about the thermal reaction of $N_2 + O_2$: thermal reaction to form either 2 NO or NNO + O is not possible. As for the direct, uncatalyzed photoreaction of N_2 with the B state of O_2, we conclude that nonadiabatic evolution to form NNO may be possible, but direct production of NO appears impossible.

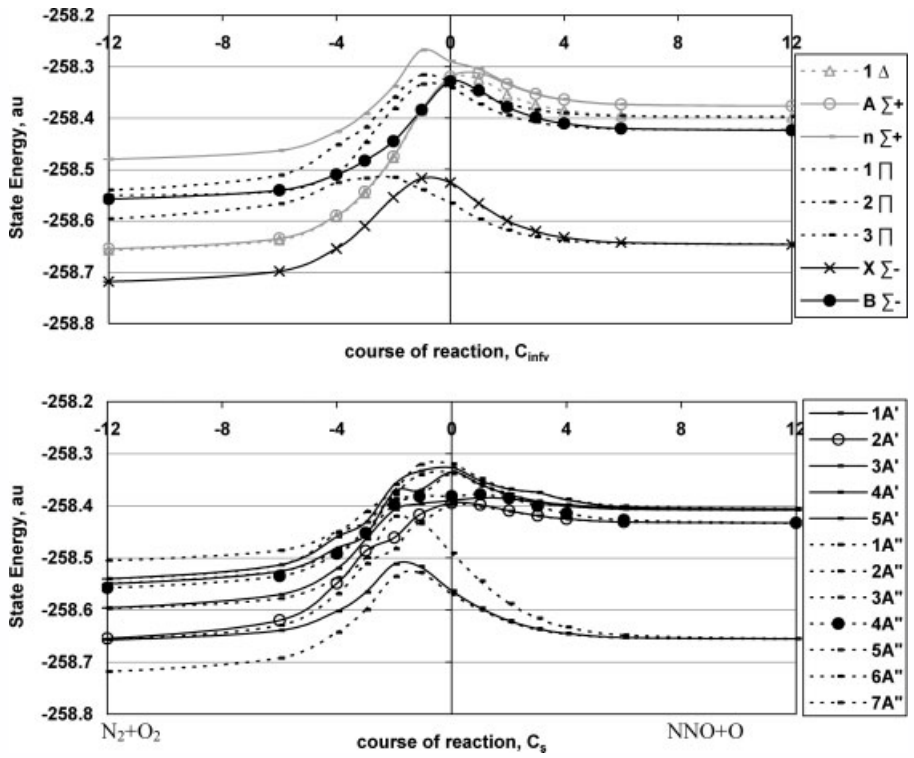

Figure 10. Computed state energies for two different $N_2 + O_2 \rightarrow NNO + O$ pathways. In both plots, the photoexcited (adiabatic) states of interest are labeled with circles (A O_2) or filled circles (B O_2).

Our conclusions could cause some concern, as they eliminate direct NO formation as an explanation for the odd-nitrogen NO_x species detected by Zipf and Prasad in their UV-induced reaction of $N_2 + O_2$.[6] Zipf and Prasad offered a modified hypothesis, in that the reaction might proceed from UV excitation of weakly-bound $N_2 \cdot O_2$ complexes.[28] Such a complex would be less bound than the NO dimer, for which the UV states appear rather like monomer states with energy splittings of only up to 1 eV.[21] Hence, the orbital and correlation plots would change very little, whether the N_2 and O_2 were considered initially complexed or separated; the only significant difference would be in the initial O—O bond length, which could alter some adiabatic (but not diabatic) state correlations. An alternative explanation for the odd-nitrogen oxides seems more likely. If prodded, we might offer as a possibility a multistep mechanism, involving first NNO production and then further reaction of nascent NNO with O or O_3, but our limited knowledge of nitrogen oxide chemistry should make this a weak hypothesis at best.

Acknowledgments

Calculations were performed on computers purchased with the assistance of the Canada Foundation for Innovation (Canada) and managed by the Laboratory of Computational Discovery (University of Regina). Preliminary work in our group by C. Seitz and K. Hunter on correlation diagram generation is acknowledged, and S. Prasad (CreativeResearch, Pleasanton, California) is thanked for suggesting the topic.

References

1. Woodward, R. B.; Hoffmann, R. J Am Chem Soc 1965, 87, 395.
2. Woodward, R. B.; Hoffmann, R. J Am Chem Soc 1965, 87, 2046.
3. Longuet-Higgins, H. C.; Abrahamson, E. W. J Am Chem Soc 1965, 87, 2045.
4. Woodward, R. B.; Hoffmann, R. Angew Chem Int Ed Engl 1969, 8, 781.
5. Buenker, R. J.; Peyerimhoff, S. D.; Hsu, K. J Am Chem Soc 1971, 93, 5005.
6. Zipf, E. C.; Prasad, S. S. Science 1998, 279, 211.
7. Prasad, S. S.; Zipf, E. C. Phys Chem Earth 2000, 25, 213.
8. Donaldson, D. J. Phys Chem Earth 2000, 25, 183.
9. Hwang, E. S.; Buijsse, B.; Copeland, R. A.; Riris, H.; Carlisle, C. B.; Slanger, T. G. J Chem Soc Faraday Trans 1997, 93, 2657.
10. Estupiñán, E. G.; Nicovish, J. M.; Li, J.; Cunnold, D. M.; Wine, P. H. J Phys Chem A 2002, 106, 5880.
11. Baker, J. J Comput Chem 1986, 7, 385.
12. Frisch, M. J.; Trucks, G. W.; Schlegel, H. B.; Scuseria, G. E.; Robb, M. A.; Cheeseman, J. R.; Montgomery, J. A., Jr.; Vreven, T.; Kudin, K. N.; Burant, J. C.; Millam, J. M.; Iyengar, S. S.; Tomasi, J.; Barone, V.; Mennucci, B.; Cossi, M.; Scalmani, G.; Rega, N.; Petersson, G. A.; Nakatsuji, H.; Hada, M.; Ehara, M.; Toyota, K.; Fukuda, R.; Hasegawa, J.; Ishida, M.; Nakajima, T.; Honda, Y.; Kitao, O.; Nakai, H.; Klene, M.; Li, X.; Knox, J. E.; Hratchian, H. P.; Cross, J. B.; Adamo, C.; Jaramillo, J.; Gomperts, R.; Stratmann, R. E.; Yazyev, Q.; Austin, A. J.; Cammi, R.; Pomelli, C.; Ochterski, J. W.; Ayala, P. Y.; Morokuma, K.; Voth, G. A.; Salvador, P.; Dannenberg, J. J.; Zakrzewski, V. G.; Dapprich, S.; Daniels, A. D.; Strain, M. C.; Farkas, O.; Malick, D. K.; Rabuck, A. D.; Raghavachari, K.; Foresman, J. B.; Ortiz, J. V.; Cui, Q.; Baboul, A. G.; Clifford, S.; Cioslowski, J.; Stefanov, B. B.; Liu, G.; Liashenko, A.; Piskorz, P.; Komaromi, I.; Martin, R. L.; Fox, D. J.; Keith, T.; Al-Laham, M. A.; Peng, C. Y.; Nanayakkara, A.; Challacombe, M.; Gill, P. M. W.; Johnson, B.; Chen, W.; Wong, M. W.; Gonzalez, C.; Pople, J. A. Gaussian 03, Revision C.02, a Software Package of *ab initio* Programs; Gaussian, Inc.: Wallingford, CT, 2004.
13. Roos, B. O.; Taylor, P. R.; Siegbahn, P. E. M. Chem Phys 1980, 48, 157.
14. Kendall, R. A.; Dunning T. H., Jr.; Harrison, R. J. J Chem Phys 1992, 96, 6796.
15. Schlegel, H. B.; Robb, M. A. Chem Phys Lett 1982, 93, 43.
16. Yamamoto, N.; Vreven, T.; Robb, M. A.; Frisch, M. J.; Schlegel, H. B. Chem Phys Lett 1996, 250, 373.
17. Werner, H.-J.; Knowles, P. J.; Schütz, M.; Lindh, R.; Celani, P.; Korona, T.; Rauhut, G.; Manby, F. R.; Amos, R. D.; Bernhardsson, A.; Berning, A.; Cooper, D. L.; Deegan, M. J. O.; Dobbyn, A. J.; Eckert, F.; Hampel, C.; Hetzer, G.; Lloyd, A. W.; McNicholas, S. J.; Meyer, W.; Mura, M. E.; Nicklaß, A.; Palmieri, P.; Pitzer, R.; Schumann, U.; Stoll, H.; Stone, A. J.; Tarroni, R.; Thorsteinsson, T. MOLPRO 2002.6, a Software Package of *ab initio* Programs; University of Birmingham: Birmingham, UK, 2002.
18. Werner, H.-J.; Knowles, P. J. J Chem Phys 1985, 82, 5053.
19. Knowles, P. J.; Werner, H.-J. Chem Phys Lett 1985, 115, 259.
20. East, A. L. L. J Chem Phys 1998, 109, 2185.
21. Levchenko, S. V.; Reisler, H.; Krylov, A. I.; Gessner, O.; Stolow, A.; Shi, H.; East, A. L. L. J Chem Phys 2006, 125, 084301.
22. Leigh, W. J.; Zheng, K.; Nguyen, N.; Werstiuk, N. H.; Ma, J. J Am Chem Soc 1991, 113, 4993.
23. Leigh, W. J. Can J Chem 1992, 71, 147.
24. van der Lugt, W. Th. A. M.; Oosterhoff, L. J. J Am Chem Soc 1969, 91, 6042.
25. Grimbert, D.; Segal, G.; Devaquet, A. J Am Chem Soc 1975, 97, 6629.
26. Olivucci, M.; Ragazos, I. N.; Bernardi, F.; Robb, M. A. J Am Chem Soc 1993, 115, 3710.
27. Lawless, M. K.; Wickham, S. D.; Mathies, R. A. Acc Chem Res 1995, 28, 493.
28. Zipf, E. C.; Prasad, S. S. J Chem Phys 2001, 115, 5703.
29. Huber, K. P.; Herzberg, G. Molecular Spectra and Molecular Structure IV: Constants of Diatomic Molecules; Van Nostrand: New York, 1979.
30. Teffo, J.-L.; Chédin, A. J Mol Spectrosc 1989, 135, 389.